

Figure S1. Co-localization of *nos* and *pgc* is detected at stage 10 and increases into early embryogenesis, Related to Figures 1 and 2.

(A-F) Confocal z-series projections at the posterior cortex of stage 10-13 oocytes and pre-cellular embryos labeled with probes for *nos* (magenta) and *pgc* (green; A-E) or *gfp* (green; F). In all images, the oocyte/embryo is oriented with posterior to the right, indicated by the asterisk in (A). (G-H) Quantification of co-localization in oocytes/embryos corresponding to (A-F). Red bars: percentage of *nos* particles detected that are co-localized with *pgc* particles (G) and *pgc* particles detected that are co-localized with *nos* (H) as a function of distance from the posterior pole; blue bars: co-localization between a non-localizing transcript, *gfp-tub-3'UTR*, and *nos* (G) or *pgc* (H). Scale bar in (A) applies to (A-F). Values shown are mean \pm S.E.M, $n \geq 4$ oocytes.

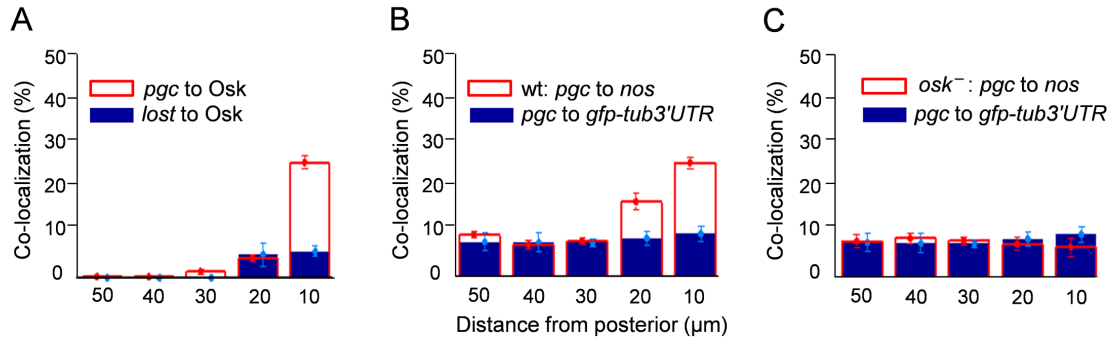


Figure S2. Co-population of granules by single *pgc* transcripts with one or more *nos* transcripts, Related to Figure 2.

(A) Quantification of co-localization of single-transcript *pgc* particles with Osk-GFP (red bars) compared to co-localization of a non-localizing mRNA, *lost*, with Osk-GFP (blue bars) as a function of distance from the posterior pole. (B, C) Quantification of co-localization of single-transcript *pgc* particles and *nos* in wild-type (red bars, B) and *osk* mutant oocytes (red bars, C) as a function of distance from the posterior pole. Blue bars show frequency of co-localization between single-transcript *pgc* particles and a non-localizing transcript, *gfp-tub-3'UTR*. Values shown are mean \pm S.E.M; $n \geq 4$ oocytes.

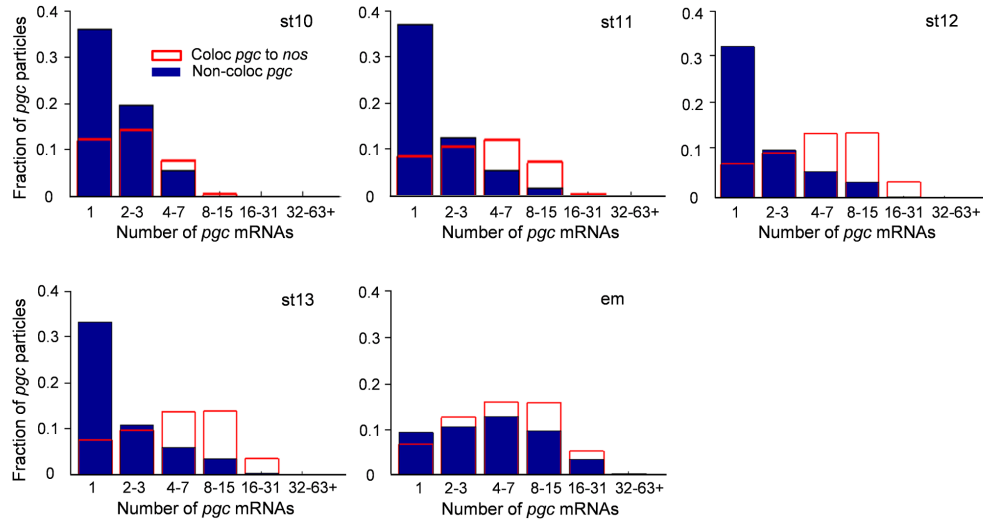


Figure S3. Growth dynamics of *pgc* homotypic clusters, Related to Figure 3.

Distribution of *pgc* particles, binned by mRNA content, that are co-localized with at least one *nos* mRNA (red bars) compared to the distribution of *pgc* particles that do not co-localize with *nos* (blue bars), from stage 10 to early embryo (em).

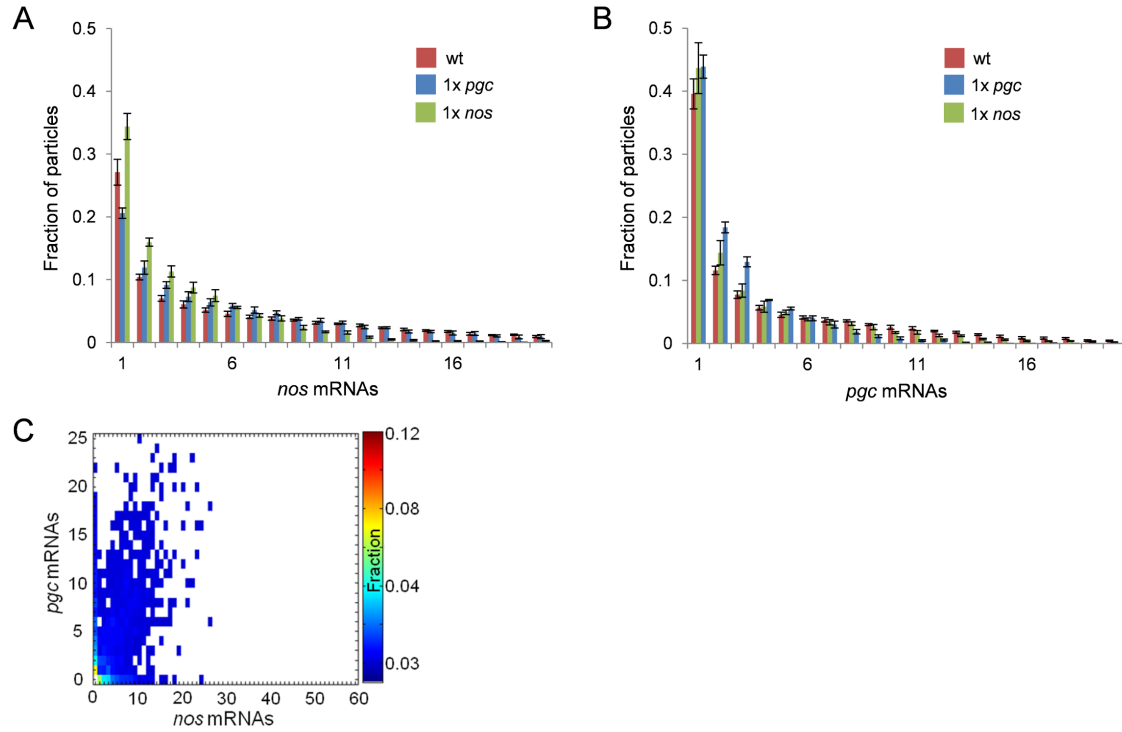


Figure S4. Effect of decreasing *nos* or *pgc* on particle size distributions, Related to Figure 5
 (A) Size distributions of *nos* particles in wild-type (wt, red), 1x *pgc* (blue), and 1x *nos* (green) oocytes. P-value for wt vs 1x *pgc* is 0.65; p-value for wt vs 1x *nos* is <.0001. (B) Size distributions of *pgc* particles in (wt, red), 1x *pgc* (blue), and 1x *nos* (green) oocytes. P-value for wt vs 1x *nos* is 0.94; p-value between wt vs 1x *pgc* is <.0001. Values shown are mean \pm S.E.M.; $n \geq 4$ stage 13 oocytes. P-values were determined using the Kolmogorov-Smirnov test (kstest2 command in Matlab). (C) Census of *nos* and/or *pgc* transcripts resident in each granule, demarcated by Osk-GFP, in stage 13 1x *nos* oocytes.

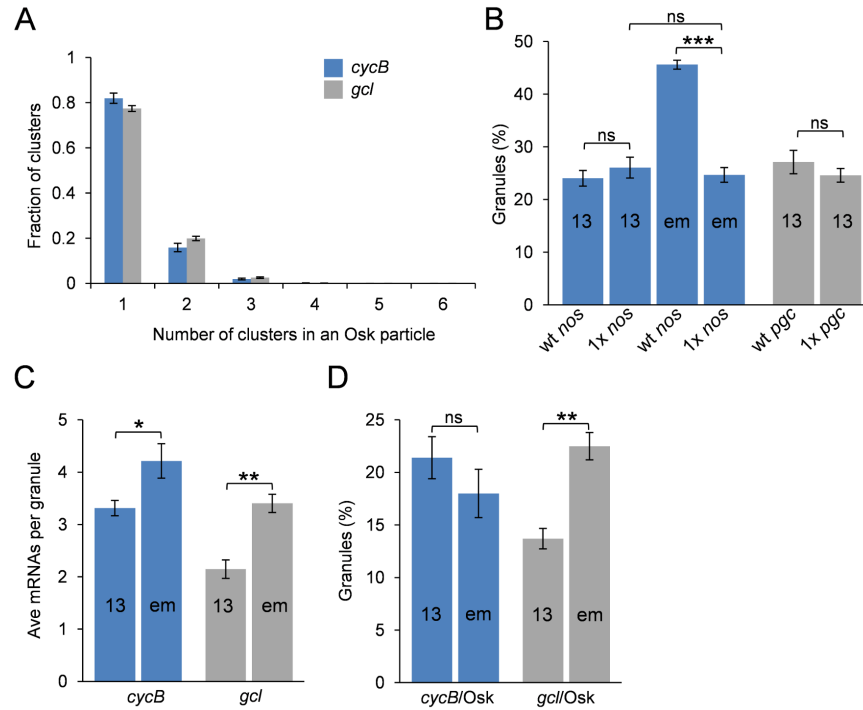


Figure S5. Additional analyses of multiple homotypic clusters, Related to Figure 6.

(A) Distributions of the number of homotypic clusters detected per germ granule (marked by Osk-GFP) in the early embryo for *cycB* and *gcl*; $n > 5$ embryos, $>6,000$ particles (B) The proportion of germ granules that contain more than one homotypic *nos* or *pgc* cluster in wild-type (wt), 1x *nos*, or 1x *pgc* stage 13 oocytes and early embryo, $n > 6$ oocytes. (C, D) Comparison of germ granule *cycB* or *gcl* content (C) and occurrence of granules with multiple *cycB* or *gcl* clusters (D) between stage 13 oocytes and early embryos. Values shown are mean \pm S.E.M. ns (not significant), $*p < 0.05$, $**p < 0.01$, as assessed by Student's t-test.